HELDA
HELSINGIN YLIOPISTO
HELSINGFORS UNIVERSITET
UNIVERSITY OF HELSINKI

UNIVERSITY OF HELSINKI

https://helda.helsinki.fi

Spatial and Temporal Patterns in Black Carbon Deposition to Dated Fennoscandian Arctic Lake Sediments from 1830 to 2010

Ruppel, Meri M.

2015-12-15

Ruppel , M M , Gustafsson , Ö , Rose , N L , Pesonen , A , Yang , H , Weckström , J , Palonen , V , Oinonen , M J & Korhola , A 2015 , ' Spatial and Temporal Patterns in Black Carbon Deposition to Dated Fennoscandian Arctic Lake Sediments from 1830 to 2010 ' , Environmental Science & Technology , vol. 49 , no. 24 , pp. 13954-13963 . https://doi.org/10.1021/acs.est.5b01779

http://hdl.handle.net/10138/326206
https://doi.org/10.1021/acs.est.5b01779

unspecified
acceptedVersion

Downloaded from Helda, University of Helsinki institutional repository.

This is an electronic reprint of the original article.

This reprint may differ from the original in pagination and typographic detail.

Please cite the original version.

Spatial and temporal patterns in Black Carbon (BC) deposition to dated Fennoscandian Arctic lake sediments from 1830 to 2010

Meri M. Ruppel,†, Örjan Gustafsson, ‡, § Neil L. Rose, ‖ Antto Pesonen, ⊥ Handong Yang, ‖ Jan Weckström, † Vesa Palonen, # Markku J. Oinonen, ⊥ Atte Korhola †*

† Department of Environmental Sciences, University of Helsinki, 00790 Helsinki, Finland

‡ Department of Environmental Science and Analytical Chemistry (ACES), Stockholm University, 106 91 Stockholm, Sweden

§ Bolin Centre for Climate Research, Stockholm University, 106 91 Stockholm, Sweden

‖ Environmental Change Research Centre, Department of Geography, University College London, London WC1E 6BT, United Kingdom

⊥ Laboratory of Chronology, Finnish Museum of Natural History – LUOMUS, University of Helsinki, 00560 Helsinki, Finland

Department of Physics, University of Helsinki, 00560 Helsinki, Finland

KEYWORDS. Black carbon, Arctic, lake sediment record, long-term trends

ABSTRACT. Black carbon (BC) is fine particulate matter produced by incomplete combustion of biomass and fossil fuels. It has a strong climate warming effect which is amplified in the Arctic. Long-term trends of BC play an important role in assessing the climatic effects of BC and in model validation. However, few historical BC records exist from high latitudes. We present five lake-sediment soot-BC (SBC) records from the Fennoscandian Arctic, and compare them with records of spheroidal carbonaceous fly-ash particles (SCPs), another BC component, for the last ca. 120 years. The records show spatial and temporal variation in SBC fluxes. Two northernmost lakes indicate declining values from 1960 to the present, which is consistent with modelled BC deposition and atmospheric measurements in the area. However, two lakes located closer to the Kola Peninsula (Russia) record increasing SBC fluxes from 1970 to the present, which is likely caused by regional industrial emissions. The increasing trend is in agreement with a Svalbard ice-core BC record. The results suggest that BC deposition in parts of the European Arctic may have increased over the last few decades, while further studies are needed to clarify the spatial extent of the increasing BC values and to ascertain the climatic implications.

1. INTRODUCTION

Black carbon (BC) particles are found globally in the atmosphere, water, snow, ice, soils and sediments (*1*). BC has both natural and anthropogenic sources from incomplete combustion of biomass, biofuels and fossil fuels (*1*, *2*). It has an atmospheric lifetime of a few days to weeks, during which it may be transported for thousands of kilometers, before being wet- or dry-deposited (*2*, *3*). BC is detrimental to human health, penetrating deep into respiratory systems and causing pre-mature deaths (*4*). In addition, it is a strong climate warming agent due to its strong visible light absorption (*2*, *3*). Globally, BC is considered to have the second most important climate warming effect after carbon dioxide (*2*, *5*).

Observations on historical BC values beyond a few decades of atmospheric monitoring are required to assess the importance of BC on past and present climate change, and for development and validation of models that are, for instance, used to produce BC emission scenarios. Such records can be reliably obtained from ice cores, marine and lake sediments and peat sequences, which contain evidence of atmospherically-deposited material in chronologically-constrained order. Some historical BC concentrations and fluxes are available from lake and marine sediments from North America (*6–12*), Europe (*13–16*) and Asia (*17–19*). These studies provide regional information on past BC fluxes, many of which concur qualitatively with historical reconstructions of fuel consumption and derived BC emission inventories (*20–21*). Overall, in North America and Europe BC fluxes increased after the mid-1800s, mostly peaking in early to middle 1900s and declined since the 1960s (*7*, *14*, *11*, *15*), whereas fluxes have increased in Asia from around 1950 to the present (*17*, *19*).

60 The climatic effects of BC are amplified in the Arctic where its deposition causes a positive
61 climate feedback by lowering the albedo of snow and ice, thereby hastening their melt due to
62 elevated heat absorption (*22–24*). Due to this feedback process BC is considered even more
63 important for Arctic warming and melting than greenhouse gases (*2*, *5*, *23*).The first observations
64 of BC in polar regions were made by Warren and Wiscombe (*25*) who found carbonaceous
65 particles darkening Arctic and Antarctic snow surfaces and continuous in-situ monitoring of
66 atmospheric BC started in the Arctic in 1989 (*26*). The amplified warming by BC in the Arctic
67 results from its deposition on highly-reflective surfaces (*2*, *23*) and so knowledge on BC
68 deposition, in addition to atmospheric measurements, is essential. However, BC deposition and
69 its concentrations in snow cannot be directly reconstructed from atmospheric BC observations as
70 at least 85-90 % of BC in the Arctic is wet-deposited (*27*) and therefore not recorded by the
71 atmospheric measurements of dry-phase BC. Furthermore, BC scavenging efficiency (i.e. wash-
72 out ratio by precipitation) may vary temporally irrespective of atmospheric BC concentrations,
73 for instance, along with varying temperatures during cloud formation (*28*). Therefore, to
74 comprehensively assess the role of BC in Arctic climate warming, the amount of BC deposition
75 is required, in addition to atmospheric measurements.

76 Historical BC loading in the Arctic has been scarcely investigated. Some observations on past
77 BC values exist in ice cores from Greenland (*29–32*) and Svalbard (*33*) but these studies indicate
78 partially differing historical BC deposition trends, as the Greenland records show slowly
79 declining or stable BC values from 1950 to the present whereas the Svalbard record indicates
80 rapidly increasing BC values from 1970 to 2004. Moreover, Greenland receives most of its BC
81 deposition from North America, and therefore high-latitude Greenland ice core trends cannot be
82 seen as representative for low-lying areas in the rest of the Arctic which receive atmospheric BC

transport mainly from Eurasia (*29*, *34*, *35*). Hence, further historical data from environmental archives are required to obtain a more reliable view on the spatial variability of past BC values in the Arctic.

Here we present BC concentrations and fluxes from five lake sediment cores in northern Finland, which represents the gateway to the high Arctic for European BC emissions. BC is an operational term and its precise definition depends on the method used for its quantification. We use the chemothermal oxidation at 375 °C (CTO-375) method, which is among the most widely used in sediment sciences, and quantifies high-refractory soot-BC (SBC) (*7*, *36*). Consequently, we use the term SBC for our specific measurements and the term BC for black carbon measurements in general, quantified by other methods. The SBC detected by the CTO-375 method are predominantly the smallest, lightest and most refractory fractions in the range of BC particles (*37*). The SBC fraction may be transported furthest in the atmosphere and is therefore applicable for studies of historical BC deposition in sediment archives of the Arctic (e.g., *15*, *37*, *38*). This study presents the first lake sediment SBC flux records from the Arctic, and compares these measurements with those previously reported for another BC component, spheroidal carbonaceous particles (SCPs) from the same lakes (*39*) to determine a tentative source analysis for the observed SBC. Together with an ice core record from Svalbard (*33*) our results represent the first attempt to synthesize the observed BC deposition/flux trends in the European Arctic between ca. 1850 and 2010.

2. MATERIAL AND METHODS

104 **2.1. Sediment Retrieval, Dating and SBC Flux Calculations**. Lake sediments were collected
105 between 2009 and 2013 from five lakes in northern Finland. These lakes (Karipääjärvi (KPJ),
106 Kuutsjärvi (KJ), Puoltsajärvi (PJ), Saanajärvi (SJ) and Vuoskojärvi (VJ)) are remote from known
107 BC sources in Finland (Fig. 1) and experience little or no direct human impact (population
108 density in the study area 0.2–0.45 inhabitants per km^{-2}). More specific information on the lakes
109 and sample collection procedure is reported in Ruppel et al. (*39*) and Supporting Information (SI,
110 Table S1). In short, surface sediment cores (top 12.5 cm) were retrieved from the deepest part of
111 the lakes with a HTH gravity corer (*40*) and subsampled at a fine resolution (0.25 cm).
112 Sediments were freeze-dried and dated radiometrically (more details in Ruppel et al. (*39*), and
113 Tables S2–S6)). The analyzed sediment is mostly the same as that used in Ruppel et al. (*39*) for
114 the analysis of SCPs, a well-defined fraction of industrial fossil-fuel combustion derived BC
115 (*41–43*), but new sediments were collected from SJ in 2013 and VJ in 2010 for SBC
116 measurements. These were not analyzed for SCPs due to lack of material.

117 Radiometric dating of the lake sediments was used to calculate depositional SBC fluxes by
118 multiplying the SBC concentration with the derived sedimentation rate (g cm^{-2} yr^{-1}). As the
119 dating uncertainty generally increases from 0–1 years in the top layers of the sediment cores to
120 20–30 years in the deepest dated samples (Tables S2–S6), it is evident that the calculated SBC
121 fluxes are most reliable for the top part of the cores.

122 **2.2 SBC Analysis.** Currently, no standard method exists to quantify all forms of BC,
123 especially in sediments. Therefore, each BC analysis method may quantify a different fraction of
124 the BC combustion continuum (e.g., *38*, *45*). The chemothermal oxidation at 375 °C (CTO-375)
125 method developed by Gustafsson et al. (*7*, *36*) is widely used for high-refractory SBC
126 quantification in soils and sediments (*37*, *38*, *46*). The method detects carbon material of high

thermal-oxidative resistance, i.e. highly condensed refractory SBC formed at high temperatures in the gas phase of combustion (*37*), and possibly some char-type BC, containing morphological features of the original fuel particle, formed at high-temperature combustion (*47*), such as SCPs (*42*). Hence, the CTO-375 method quantifies the most condensed forms of BC, irrespective of their source (e.g., biomass or fossil fuel) (*38*). Char-BC particles formed at lower combustion temperatures (i.e. less condensed forms of BC) have lower thermal-oxidative stabilities and have lower recovery with the CTO-375 method (*37*). The CTO-375 method has also been shown to effectively exclude highly condensed and potentially interfering non-BC organic matter such as wood, melanoidin and pollen and thus avoids false positives (*7*, *37*, *38*, *46*).

Dried sediments were ground to less than 100 μm with a stainless steel ball grinder (Retsch, Mixer Mill 4000). Approximately 10 mg of sediment was weighed precisely into pre-combusted (12 h at 450 °C) silver capsules (5 × 8 mm), and combusted in a custom-made tube furnace at 375 °C for 18 hours under active airflow (200–300 mL min^{-1}), to oxidize organic material. Subsequently, carbonates were removed by in-situ microscale acidification with 1M HCl. Lastly, the residual carbon content was quantified as SBC with a Flash 2000 Organic Elemental Analyser (Thermo Fisher) (at 1050 °C) along with nitrogen (N) measurements. As the concentration of SBC was expected to be very low, extreme care was undertaken in the production of a calibration curve for the elemental analyzer with standardized reference material of known (total) carbon content, supplied by the device manufacturer. In each analytical run (max. 32 samples), 5–6 soil reference standard samples of known carbon and nitrogen content (Thermo Fisher) were included to determine the reliability and repeatability of the analysis.

While the CTO-375 method has been demonstrated to have a lower potential to give false positives for non-BC condensed organic matter compared to other methods (*36*, *38*, *46*), there is

always a risk of charring. To evaluate the charring potential of the samples, the non-soot organic carbon (NS-OC) content of the samples was determined. Approximately 10 mg of each, or each alternate, sample from each sediment core was weighed into silver capsules and acidified with 1M HCl, as above. The total organic carbon (TOC) content was quantified with the elemental analyzer and the NS-OC content of the samples determined by subtracting the amount of SBC from the TOC values. Studies have shown TOC and BC values to correlate (e.g. *38*), and as SBC is only a fraction of total BC present in sediments and a large portion, namely char-BC, remains in the NS-OC, positive correlations may be expected between SBC and NS-OC without this being evidence of charring. In addition, while an absence of a positive NS-OC-SBC relationship is supportive of the absence of significant charring, the presence of such a relationship may not be taken as evidence for charring, as NS-OC and SBC may be co-sorted with the fine fraction in sediments. For instance, while a correlation between NS-OC and SBC was recorded in North American sediments, SBC could much better explain the spatial distribution of similarly combustion-derived PAHs than NS-OC (*7*, *8*). Furthermore, also high (> 1 mass %) nitrogen content of sediment samples bear the potential for charring as nitrogen-containing macromolecules have been shown to char during the CTO-375 pretreatment and cause a positive bias to BC measurements (*48*). The nitrogen content of the samples was automatically determined during the elemental analysis.

2.3 Uncertainties. Evaluation of the method accuracy and precision is described in more detail in SI. In short, as no standard reference material of BC exists (*38*), the accuracy of the method can only be evaluated by comparing SBC results from selected standard reference material reported in previous studies using the same or similar methods. Our (and literature) results of SBC and TOC concentrations in five standard reference materials are presented in Table S7. Our

SBC results were within one standard deviation of published mean data with the exception of one reference material (details in SI). Importantly, no SBC was quantified in the wood char that contains high amounts of OC but no SBC, indicating that oxygen supply during the oxidation phase was sufficient to avoid charring.

The most reliable estimate of the method precision (relative standard deviation) is 2.24 % which was ascertained by duplicate to quintuple analyses of sediment samples, and 23 repeated measurements of a soil reference material. Furthermore, to illustrate the repeatability of the method and specifically the reported temporal trends of SBC fluxes, subsamples of the SJ samples and the majority of VJ samples were prepared and analyzed twice for SBC (Fig. S1).

3. RESULTS AND DISCUSSION

3.1 SBC, NS-OC and N Concentrations. NS-OC concentrations varied from ca. 0.05 g gDw^{-1} (gram per gram dry weight) to ca. 0.25 g gDw^{-1}, and SBC concentrations from 0.6 mg gDw^{-1} to 5.1 mg gDw^{-1} in the lake sediment samples (Fig. S1). Lowest SBC concentrations were measured in SJ, and highest in KJ. The SBC / NS-OC ratio was ca. 0.01–0.02 in KPJ, PJ, SJ and VJ, and 0.02–0.04 in KJ. As the SBC / NS-OC ratio is very low, even relatively little charring of NS-OC during the oxidation phase may potentially significantly affect the SBC concentrations. The NS-OC and SBC values showed significant *positive* correlation in two cases out of five (KPJ and KJ) (Fig. S1). This may relate to SBC and NS-OC being co-sorted in the sediments, and also char-BC being part of NS-OC. As charring during the sample preparation is unlikely for the other lakes (PJ, SJ and VJ), and as the standard reference material analyses (Table S7) indicated no charring, charring is also considered unlikely for KPJ and KJ. In addition, the nitrogen

content of all samples was below the detection limit of the elemental analyzer (0.01 mass %), which further supports the absence of charring (*48*).

3.2 SBC Fluxes and Sediment Focusing. As SBC represents only a minor sediment component, its concentrations may be strongly affected by varying inputs of other sediment material that may concentrate or dilute it. Therefore, the SBC data is reported as depositional fluxes (Fig. 2A, B) taking into account any variations in sedimentation rates in addition to the observed concentrations. As the calculation of fluxes is constrained by the radiometric dating using excess ^{210}Pb (half-life of 22.3 years), fluxes cannot be presented beyond ca. 120–150 years (Tables S2–S6).

To our knowledge, these are the first depositional SBC fluxes reported for the Arctic. Fluxes varied from ca. 0.02 to 0.5 g m^{-2} yr^{-1} (Fig. 2A) and the lowest values are considerably (1–2 orders of magnitude) lower than previously reported SBC fluxes from alpine lakes in Slovenia and Switzerland (*13*, *15*), but of the same order as reported by Elmquist et al. (*14*) from rural southern Sweden. The majority of the SBC fluxes are below 0.1 g m^{-2} yr^{-1}, which is similar to preindustrial and lowest 20th century values in Elmquist et al. (*14*), but PJ, and particularly KJ, show some notably higher fluxes than these (Fig. 2A, B). We consider that the high KJ fluxes prior to 1900 (2-4 times higher than other lakes) are unlikely to represent true atmospheric SBC deposition as no BC source of sufficient local influence is likely to have existed at this time. This discrepancy between KJ and the other lakes is likely an artefact of the steeply funnel-shaped catchment area of KJ and sediment focusing where re-suspended sediment in the littoral zone moves to deeper accumulating zones of the lake (*49*). In KJ, sediment focusing is a consequence of steep lake bathymetry, and is evidenced by several times higher unsupported ^{210}Pb fluxes in the core compared to the other study lakes (Table S2–S6). Despite sediment focusing, the dating

of the KJ core seems robust (Table S3). This implies that the SBC flux *trend* in KJ is reliable but absolute values are elevated. None of the other study lakes is significantly affected by sediment focusing as lakes with simple/smooth bathymetries were favored during selection. However, due to possible minor effects of material influx from the catchment area to the coring locations (*49*), it is not possible to infer exact atmospheric SBC deposition from the sediment SBC fluxes presented in Fig. 2. As individual SBC flux trends could potentially be affected by external factors, such as delayed SBC export from the catchment area or dating biases, only recurring features of the temporal SBC trends in more than one lake should be considered important.

3. 3 SBC vs SCP Flux Trends. The observed temporal trends in SBC fluxes indicates considerable differences between sites (Fig. 2 A, B), despite SCP fluxes showing clear recurrent patterns at KPJ, KJ, PJ and SJ (*39*; Fig. 2C). The SCP records are robust and show similar temporal patterns across Europe with fluxes increasing rapidly from the 1950s as a result of increased coal and oil based energy consumption and industrial production after World War II (*50*). SCP fluxes peaked in the 1970s to 1980s and then declined to the present due to improved particle arrestor technology, increased use of natural gas rather than coal, and regional declines in heavy industry (*42*, *51*, *52*). However, according to our results SCPs represent a minor fraction of SBC, as the mass ratio of SCPs to SBC is at most 0.01 to 0.02 (cf. Fig. 2B, C). Despite SBC having significant sources that do not produce SCPs, such as natural gas combustion, diesel and gasoline engines, and wildfires, the SBC and SCP flux trends do show positive correlations, of which some are significant (in KPJ, $r = 0.43$, $p = 0.061$; in KJ, $r = 0.76$, $p < 0.001$; in PJ, $r = 0.61$, $p < 0.001$). This implies the potential for source identification of SBC with the help of SCPs, as discussed below. By contrast, SBC fluxes in SJ and VJ do not seem closely linked to

240 the general SCP pattern over Europe, which may suggest that SBC transport and deposition to
241 the study lakes is more complex than that of SCPs.

242 **3.4 Varying SBC Flux Trends.** Previous studies on historical SBC fluxes to lake sediments
243 using the CTO-375 method (or a variation thereof) have indicated both regional similarities in
244 trends (*7*, *10*) and significant differences (*13*, *15*) between sites. Three urban lake sediment cores
245 in eastern North America showed similar trends with soot/graphitic BC fluxes starting to
246 increase significantly around 1950 reaching peak values in 1960–1970 and a subsequent decrease
247 (*7*, *10*), whereas records from mostly alpine lakes in Slovenia and Switzerland showed both
248 similarities and significant differences in temporal SBC fluxes within these regions (*13*, *15*). The
249 discrepancies in SBC fluxes within a comparatively small area are most likely due to varying
250 atmospheric transport patterns to the sites (*13*, *15*), or possibly differences in lateral flux of SBC
251 from the catchment areas to the lakes.

252 Trends in our study lakes seem to indicate regional patterns in SBC fluxes. The two
253 northernmost lakes, SJ and VJ, show similar temporal trends, as do the two lakes (KJ and KPJ)
254 located closest to the Kola Peninsula (Fig. 3B, C). The trends in SJ and VJ SBC fluxes are
255 characterized by small peaks around 1910 and 1960 with VJ fluxes decreasing throughout the
256 record, and SJ fluxes dropping rapidly to lower levels after 1960 (Fig. 3B). These sediment SBC
257 trends show similar features to historical BC emission inventory data from OECD Europe
258 derived by applying emission factors to fuel consumption data (*21*), as well as modelled annual
259 anthropogenic BC deposition trends at SJ between 1900 and 2010, determined using a chemical
260 transport model (OsloCTM2, data from Ruppel et al. (*39*); Fig. 3A). Generally, the drop in BC
261 emissions and modelled BC deposition after 1960 is caused by implementation of "Clean Air"
262 legislation and technological advances, e.g. increased combustion efficiency or changes in fuel

types of industrial facilities (e.g. *21*). In addition, the observed SBC flux at SJ drops rapidly around 1960 (Fig. 3B). SJ has been shown to be highly susceptible to pollution transported from Kiruna (*39*), an iron ore mine in northern Sweden, and possible changes carried out at this facility may have partly contributed to the observed drop in SBC fluxes around 1960. However, the rapid drop of the SJ SBC fluxes may be exaggerated by a sudden change in the sedimentation rate of the sediment core around 1960 (Table S5), and the drop may in reality have been more gradual, as indicated by the SBC concentration trend of SJ (Fig. S1). At VJ, the expected drop in SBC fluxes since 1960 may have been subdued by the opening (and subsequent emissions) of a large nickel, palladium, and copper mine and smelter in 1946 at Nikel on the Kola Peninsula, Russia, only ca. 150 km away from VJ (Fig. 1). SBC fluxes at VJ drop rapidly in the late-1990s at the same time as significant sulphur dioxide (SO_2) emission reductions were achieved at this facility (*53*). The declining trend in the model results after 1960 (Fig. 3A, B), and observed later in the VJ record, are further supported by atmospheric BC measurements at VJ indicating a 78 % drop in atmospheric BC concentrations from 1971 to 2011 (*54*). However, lake sediment SBC flux trends should be compared cautiously to emission from any individual potential BC source as the SBC records are expected to reflect a complex end result of BC emissions in Europe and the former USSR, short- and long-distance atmospheric BC transport, temporal variation of BC scavenging efficiency, and various catchment and sediment processes potentially affecting the recorded SBC fluxes. Therefore, SBC flux trends notable in more than one sediment record are expected to portray regional patterns.

Unfortunately, no reliable dating is available for the SJ and VJ sediment cores prior to 1874 ± 30 and 1879 ± 16 respectively, making a comparison of flux data prior to that time impossible. However, it is expected that the SBC flux to the lakes was lower in pre-industrial times before

1850, as suggested by extrapolated SBC fluxes in SJ (Fig. S2) , which results in a further similarity between the observed SBC fluxes and the model and emission inventory results prior to 1900. Both sediment records show high BC values around 1880 (Figs. 3B, S2) that are not captured by the model deposition or emission data. However, SBC fluxes similar to those of the 20th century were also seen in ca. 1870 in southern Swedish sediments (*14*) and also in elemental carbon (EC) deposition in a Svalbard ice core (Fig. 4B and highlighted in Fig. S2), suggesting that pre-industrial SBC values may be recorded only prior to 1850. Moreover, the observed SBC fluxes incorporate BC deposition caused by natural fires which are not captured by the emission inventories or modelling results but contribute to BC values in the Arctic (e.g. *2*, *24*), particularly in time periods preceding modern fire prevention, which may further explain early discrepancies.

The SBC fluxes to the SJ and VJ sediments are almost an order of magnitude higher than the deposition indicated by the model results for the area (Fig. 3A, B). This difference seems large, especially as SBC is a component of total BC, and the model results aim to include the whole continuum of soot and char-type BC. However, it is known that models underestimate BC concentrations in the Arctic (*54–56*), and specifically the OsloCTM2 model has shown a factor of 10 lower snow BC concentrations in the European Arctic than observed in snow measurements (*57*). Moreover, in remote areas SBC may dominate overall BC fluxes as it is the BC fraction transported furthest due to its low mass (e.g., *15*).

As presented in Figure 3C, the temporal trends of SBC flux in KPJ and KJ also show evident similarities. Both show comparably little variation from the beginning of the records to ca. 1970 when a notable increase in SBC fluxes commences and continues to the end of the records (2013 and 2005 respectively). Although the KJ record shows a different trend to SJ and VJ after ca. 1950, prior to this it shows clear similarities (Figs. 3B, C, S2). Consequently, the data suggests

309 that the fluxes depicted by SJ and VJ (and KJ prior to 1950) may present a general SBC trend in
310 the region upon which differing (locally to regionally-influenced) flux components are
311 superimposed. The increase in SBC flux after ca. 1970 observed in KPJ and KJ is most likely
312 caused by contamination from the Kola Peninsula, Russia. The region is rich in various ores and
313 minerals and is one of the most industrially developed regions in northern Russia. A small
314 mining city, Kovdor, is located only ca. 30 km east of KJ, but several other mining loci,
315 including Monchegorsk, one of the most severely polluted cities in Russia, and a large port city,
316 Murmansk, are located within a 200 km radius (Fig. 1B). The fact that KJ, as opposed to the
317 other lakes, records higher SCP fluxes in the 1990s and 2000s than during the geographically
318 widespread 1980s peak (Fig. 2C), suggests that the observed increasing SBC flux post-1970 may
319 (at least in KJ) be caused by industrial emissions. Intermittent and recurring winds from east to
320 south-east transport pollution from the Kola Peninsula primarily to KJ and KPJ (39; Fig. S3).
321 Other potential sources could be increasing BC emissions from the transport sector in western
322 countries (*2*) or from flaring in north-western Russia (*57*, *58*), but BC deposition from such long-
323 distance sources would be expected to be observed at all of our study lakes. We can only
324 speculate on the reason for the increasing flux beginning in ca. 1970 in KJ and KPJ as no precise
325 information on BC emissions, and particularly their temporal trend, from the various facilities on
326 the Kola Peninsula are available (*56*), but the fact that the trend is clearly recorded at two
327 locations ca. 200 km apart, increases its plausibility and suggests the source to be regional as
328 opposed to local.

329 The terrestrial area affected by Kola Peninsula emissions seems to be at least ca. 100 000 km^2,
330 as the closest plausible emission sources are located at 150–200 km from the lakes (KJ and KPJ).
331 It is surprising that the pollution is not more notable at the VJ located close to Nikel (Fig. 1), but

the emissions from Nikel are likely transported more efficiently to the north (i.e. Arctic Ocean) than west to VJ (Fig. S3; *54*). Studies of 32 lakes on the Kola Peninsula indicated the effect of anthropogenic sulphur and heavy metal emissions to be surprisingly geographically restricted and controlled mainly by the surrounding topography and prevailing winds (*60*). Consequently, it seems that the differences in long-term SBC flux trends observed in SJ and VJ compared with KPJ and KJ may be caused by them partially receiving different general atmospheric transport, but possibly also local (e.g. topography-related) differences in their receptivity to pollution originating from the Kola Peninsula.

The SBC record observed in PJ presents another different SBC trend (Fig. 2A). Although previous studies have also recorded variable SBC fluxes between different lakes within a region (*13*, *15*), the specific cause of the trend in PJ remains unclear. However, it is dominated by a strong increase in SBC fluxes from the start of the record in 1892 ± 20 to 1948 ± 8 (Fig. 2A), which is not evident in the concentration trend (Fig. S1), and is thereby driven by a strong increase in sediment accumulation rates. However, the early chronology has large uncertainties in the radiometric dating (Table S4) and therefore the fluxes in PJ from 1892 to 1948 must be considered tentative.

Previous studies have associated the temporal trend of SBC fluxes in sediments to the history of fuel use and technological advances in combustion (*10*, *14*, *17*). In the case of three urban lake sediments from eastern North America the timing of peaking BC fluxes contrasted dramatically with the estimated history of BC emissions in North America (*10*; emission data from Bond et al. (*21*)). Our data show within a restricted region both SBC flux records that match estimated historical BC emission data and modelled BC deposition (SJ and VJ), as well as records contrasting these (KJ, KPJ and PJ), which are most likely connected to those receiving different

355 atmospheric transport, particularly from regional emission sources such as the industrial facilities
356 on the Kola Peninsula.

357 **3.5 Synthesis of SBC Flux Trends, Comparison with a Svalbard Ice Core EC Record and**
358 **Implications for the Arctic.** To assess whether a general trend of SBC flux could be extracted
359 from these partly contrasting records, four SBC flux records (KPJ, KJ, SJ and VJ) were
360 standardized (by subtracting the mean and dividing by the standard deviation) and a LOESS
361 smoother (span = 0.15; method using locally weighted regression to smooth data) fitted to the
362 stacked standardized data (Fig. 4A). The sediment records were standardized and the smoother
363 run only for time intervals for which SBC flux data was available from all the lakes, so that no
364 single record could dominate the smoothed trend. Such analysis is reasonable when the natural
365 background level of atmospheric SBC fluxes is unknown and it is impossible to assess whether
366 the actual magnitude of atmospheric SBC fluxes has varied between the lakes, and therefore only
367 the relative trends in SBC fluxes can be meaningfully scrutinized. PJ was left out of the analysis
368 due to its potentially dating-biased trend. The standardized smoothed SBC trend shows a peak in
369 fluxes around 1910 and decreasing fluxes thereafter, only shortly interrupted by a small peak
370 before 1960. Fluxes increased again starting in ca. 1970 with highest values reached in the late
371 1990s (Fig. 4A). These four SBC flux records are certainly too few to generate a reliable general
372 trend for past atmospheric SBC deposition in the study region, but they may indicate increasing
373 BC deposition from ca. 1970 to the present in some parts of the European Arctic. Notably, the
374 smoothed synthesis trend of the four SBC records shows similar features between 1850 and 2010
375 with an elemental carbon (EC, a thermal-optical proxy for BC) ice core record from Svalbard
376 (Fig. 4B; *33*). The ice core trend is not affected by local pollution (see discussion and references

377 in *33*) and the increase in EC deposition between 1970 and 2004 is most likely caused by flaring
378 emissions from northern Russia (around the Yamal Peninsula) (*33*).

379 Until now, it has been widely believed that BC concentrations and deposition have been
380 declining in the Arctic. Atmospheric measurements from Arctic observation stations at Alert
381 (Canada), Barrow (Alaska), and Ny-Ålesund (Svalbard) have indicated a 40 % decline in
382 atmospheric BC concentrations from 1990 to 2009 (*26*), in addition to the declining atmospheric
383 concentration trend measured in northern Finland at VJ (*54*). Ice core data from Greenland
384 recorded decreasing BC concentrations and deposition from peak values around 1910 to almost
385 pre-industrial levels after 1950 (*29–32*). In addition, various modelling exercises have indicated
386 declining atmospheric and snow BC concentrations and deposition from around 1960 to the
387 present, at several locations in the Arctic (*39*, *54*, *61*, *62*). Here, two of the study lakes (SJ and
388 VJ) record declining SBC fluxes since ca. 1960, in agreement with model results from the region
389 (*39*, *61*). However, two of the study lakes (KPJ and KJ) indicate increasing SBC fluxes from ca.
390 1970 to the present, in agreement with the EC ice core record from Svalbard (Figs. 4, S2). As
391 increasing values of different BC components are recorded separately, both in an area *not*
392 affected by local pollution (Svalbard) (*33*), as well as in areas where local to regional pollution is
393 plausible (KPJ and KJ), the general BC deposition trend in some parts of the European Arctic
394 may have been increasing over the last few decades, although this trend needs to be verified with
395 other records of higher spatial resolution. Based on the available data it is not currently possible
396 to confirm how geographically representative either the increasing or the decreasing BC trend is.
397 While our data substantially contribute to knowledge on historical BC deposition in the
398 European Arctic, past BC deposition data is still missing from most of the Arctic, including
399 Siberia and North America. Our data supports the hypothesis that BC deposition trends observed

400 at the high-elevation Greenland sites receiving pollution mainly from North America cannot be
401 seen as representative for other parts of the Arctic receiving atmospheric transport mainly from
402 Eurasia. They also emphasize that atmospheric BC measurements do not necessarily indicate the
403 full pattern of the BC burden in the Arctic, and both observations of atmospheric concentrations
404 and surface deposition are needed to fully assess the climate impact of BC in the area. In
405 addition, our results suggest that while BC deposition data is lacking from most of the Arctic,
406 such deductions as made in the AMAP (*24*) report of the Arctic substantially warming during the
407 last 20 years despite decreasing BC concentrations, may be premature. Regardless of the specific
408 causes for the observed increasing BC flux and deposition trends in two of our studied lake
409 sediment records and the Svalbard ice core, our results suggest that BC may have exerted a
410 significant impact on the radiative forcing and thereby past climate warming of at least some
411 parts of the European Arctic in the most recent three or four decades.

412 Based on these data, it would appear that temporal trends in BC deposition may differ
413 significantly on a small spatial scale such that observations cannot easily be extrapolated over
414 wider areas. Further observations are needed to clarify the effect of industrial development
415 within the Arctic on BC values and resulting climate forcing in the region. We have not
416 attempted exhaustive source apportionment of the observed SBC and further investigations to
417 determine the source of observed BC, e.g. by radiocarbon apportionment (*63*), are desirable. BC
418 emissions are expected to increase in the Arctic in the future as economic development (e.g.,
419 shipping and oil and natural gas extraction) is facilitated by the retreat of the Arctic Ocean sea
420 ice. The potential for detrimental effects due to such developments is underlined by observations
421 that BC emitted within the Arctic generates an almost five times higher Arctic surface
422 temperature response when compared with BC emitted at mid-latitudes (*64*). At present BC

emissions within the Arctic may be much more pronounced than presumed, as natural gas flaring in northern Russia in connection to oil and gas extraction may contribute up to 42 % of annual mean surface BC concentrations in the Arctic (*59*), a proportion which has previously been greatly underestimated or disregarded in historical emission inventories (such as Bond et al. (*21*)) and consequently also in modelling studies (*56*, *59*). Huang et al. (*56*) present the first regional BC emission inventory specifically developed for Russia for the year 2010, and show that 36.2 % of total Russian anthropogenic BC emissions result from gas flaring. The extent of the area affected by these and other potentially underestimated BC emissions, such as those on the Kola Peninsula, remains to be determined by atmospheric, snow and environmental records. Therefore, while observations of declining BC values in the Arctic are politically attractive, the growing number of records indicating increasing BC values, suggest that further data are required to resolve both temporal trends and spatial variability of BC deposition within the Arctic. These are important in order to guide future mitigation policy.

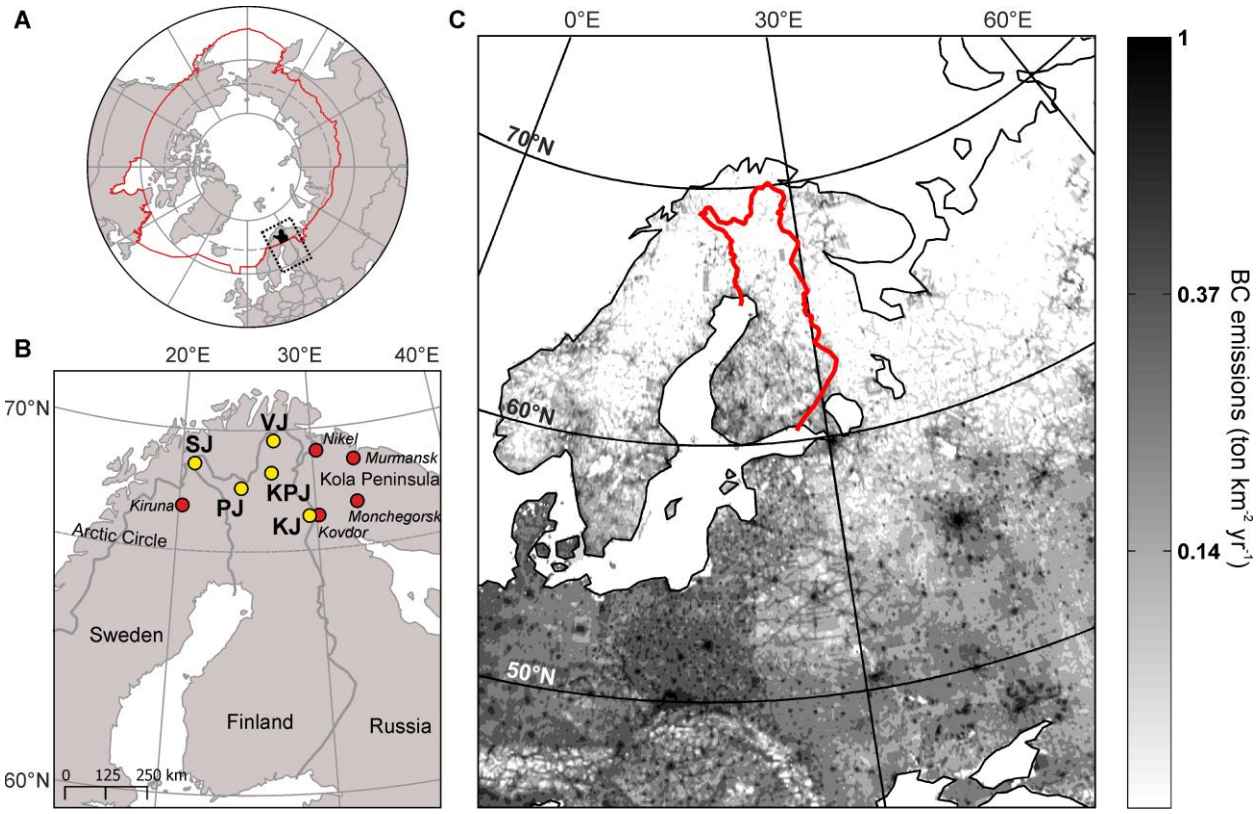

Figure 1. Geographical location of the study area and research sites within the Arctic, and BC emission sources and strengths. A) A map of the Arctic showing the definition of the Arctic by AMAP (*red line*). The study area in arctic Finland is highlighted in black. B) Locations of study lakes (*yellow dots*), and potential significant emission sources for the study lakes (*red dots*). C) Modelled annual anthropogenic BC emissions (ton km^{-2} yr^{-1}) in 10-km resolution in the vicinity to the study area, data from Wang et al. (*44*). The study area receives atmospheric transport mostly from the south (*39*; Fig. S3). The terrestrial border of Finland is shown in red.

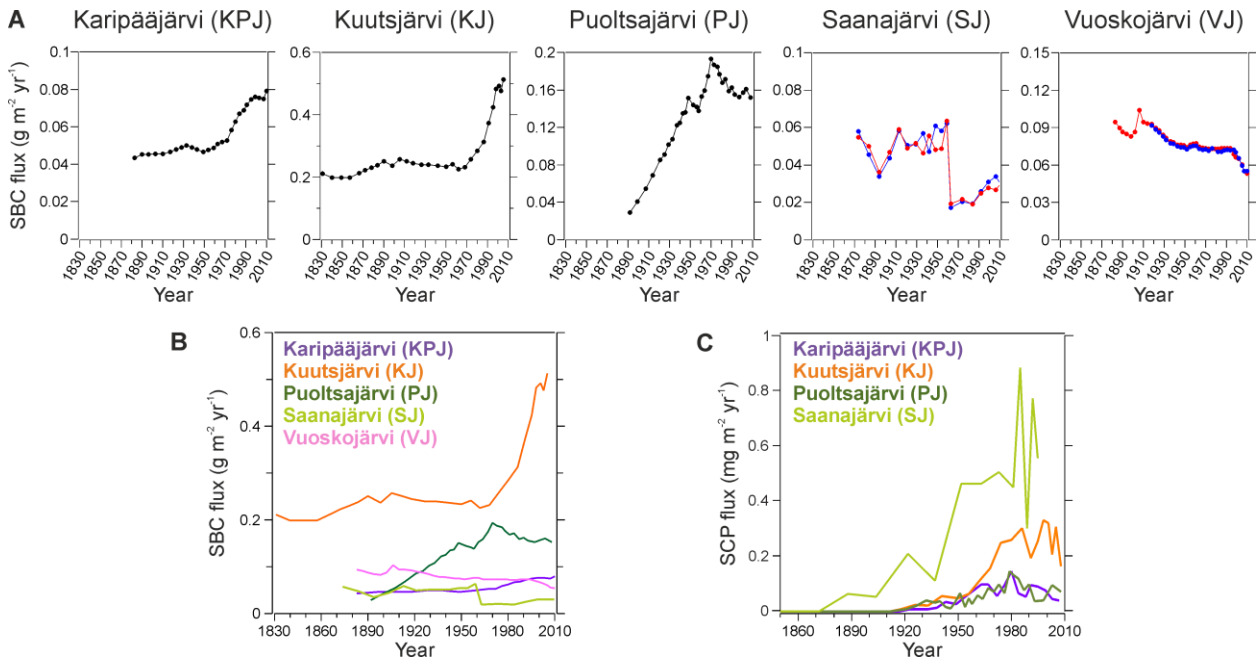

452

453 **Figure 2.** Soot black carbon (SBC) and spheroidal carbonaceous particle (SCP) fluxes (g m^{-2} yr^{-1}
454 and mg m^{-2} yr^{-1}, respectively) to the study lakes. A) SBC fluxes for each lake separately. Note
455 the different y-axis scales. Red and blue in SJ and VJ indicate separate duplicate sample analysis
456 runs. B) SBC fluxes for all lakes. The results for SJ and VJ are the averages of the duplicate
457 samples. C) SCP fluxes to KPJ, KJ, PJ and SJ, data from Ruppel et al. (*39*).

458

459

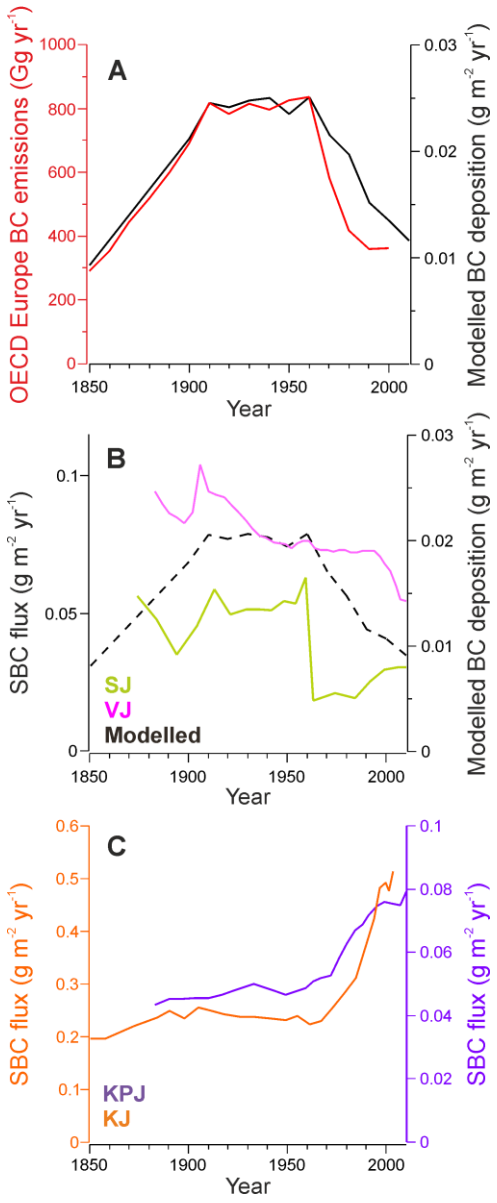

460

461 **Figure 3.** Historical BC emissions compared to modelled BC deposition in the study area, and
462 SBC fluxes SJ, VJ, KPJ and KJ. A) Red: historical annual anthropogenic BC emissions in Gg yr^{-}
463 ^{1} in OECD Europe, data from Bond et al. (*21*). Black: modelled mean annual anthropogenic BC
464 deposition at KPJ, KJ, PJ and SJ, data from Ruppel et al. (*39*). B) SBC flux at SJ and VJ
465 compared to modelled annual anthropogenic BC deposition at SJ (g m^{-2} yr^{-1}). C) SBC flux (g m^{-2}
466 yr^{-1}) at KPJ and KJ. Note that the y-axis scales are different for KJ and KPJ.

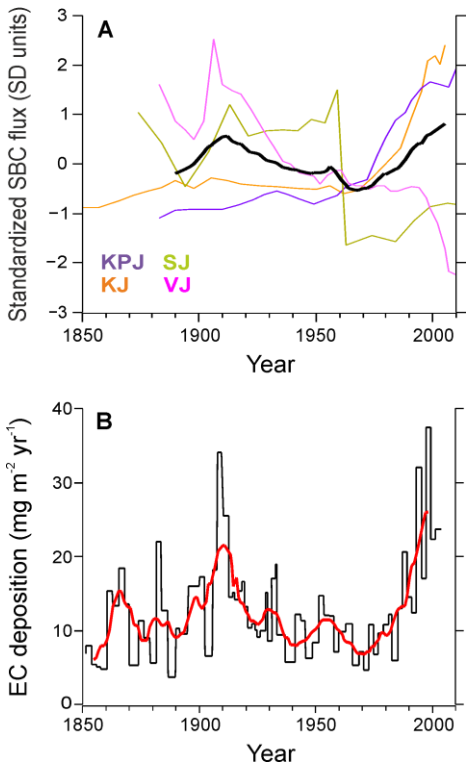

Figure 4. Standardized SBC fluxes to KPJ, KJ, SJ and VJ compared to EC deposition to a Svalbard ice core. A) Stacked SBC fluxes at KPJ, KJ, SJ and VJ expressed as standard deviations from the mean. Black curve = LOESS smoother (span = 0.15) of time intervals from which data is available from all included lakes. B) Elemental carbon (EC) deposition (mg m^{-2} yr^{-1}) to Holtedahlfonna glacier in Svalbard with 10-year running averages (*red curve*) (data from Ruppel et al. (*33*).

Supporting Information. The Supporting Information includes: tables of site description and radiometric dating of lake sediment cores; an assessment of method accuracy and precision; a table of total organic carbon (TOC) and soot black carbon (SBC) results of standard reference material; a Figure on the non-soot organic carbon (NS-OC) and SBC concentrations in the lake sediments and their correlations; a Figure on observed and cautiously extrapolated (beyond dated sediment layers) SBC fluxes compared to Svalbard ice core EC deposition; and a Figure on air mass transport to the study area. This material is available free of charge via the Internet at http://pubs.acs.org.

Corresponding Author

* Meri M. Ruppel, Department of Environmental Sciences, P.O. Box 65, FI-00014 University of Helsinki, Finland. Phone: +358-50-4486481, Fax: +358-9-191 57788, E-mail: meri.ruppel@helsinki.fi

ACKNOWLEDGMENTS

The research was funded by the Academy of Finland grant 257903. In addition, support by the NordForsk Top-level Research Initiative Nordic Centre of Excellence CRAICC, Finnish Cultural Foundation, Emil Aaltonen Foundation, and University of Helsinki Heinonsalo Fund is highly acknowledged. J.S. Salonen is thanked for technical assistance with GIS and R, August Andersson for Figure 1C, and H. Turunen for help with the TOC measurements.

ABBREVIATIONS

BC, black carbon; SBC, soot black carbon, CTO-375, chemothermal oxidation at 375 °C; SCP, spheroidal carbonaceous particle; NS-OC, non-soot organic carbon; EC, elemental carbon

REFERENCES

1. Goldberg, E. D. *Black carbon in the environment*; John Wiley and Sons: New York, USA, 1985.

2. Bond, T. C.; Doherty, S. J.; Fahey, D. W.; Forster, P. M.; Berntsen, T.; DeAngelo, B. J.; Flanner, M. G.; Ghan, S.; Kärcher, B.; Koch, D.; Kinne, S.; Kondo, Y.; Quinn, P. K.; Sarofim, M. F.; Schultz, M. G.; Schulz, M.; Venkataraman, C.; Zhang, H.; Zhang, S.; Bellouin, N.; Guttikunda, S. K.; Hopke, P. K.; Jacobson, M. Z.; Kaiser, J. W.; Klimont, Z.; Lohmann, U.; Schwarz, J. P.; Shindell, D.; Storelvmo, T.; Warren, S. G.; Zender, C. S. Bounding the role of black carbon in the climate system: A scientific assessment. *J. Geophys. Res.–Atmos.* **2013**, *118*, 1–173; DOI 10.1002/jgrd.50171.

3. Ramanathan, V.; Carmichael, G. Global and regional climate changes due to black carbon. *Nature Geosci.* **2008**, *1*, 221–227; DOI 10.1038/ngeo156.

4. WHO. Review of evidence on health aspects of air pollution – REVIHAAP Project, Technical Report **2013**, World Health Organization Regional Office for Europe, Copenhagen, Denmark, 309 pp.

5. Jacobson, M. Z. Strong radiative heating due to the mixing state of black carbon in atmospheric aerosols. *Nature*, **2001**, 409, 695–697; DOI 10.1038/35055518.

6. Goldberg, E. D.; Hodge, V. F.; Griffin, J. J.; Koide, M.; Edgington, D. N. Impact of fossil fuel combustion on the sediments of Lake Michigan. *Environ. Sci. Technol*. **1981**, 15, 466–471.

7. Gustafsson, Ö.; Haghseta, F.; Chan, C.; Macfarlane, J.; Gschwend, P. M. Quantification of the dilute sedimentary soot phase: Implications for PAH speciation and bioavailability. *Environ. Sci. Technol.*, **1997**, *31* (1), 203–209.

8. Gustafsson, Ö.; Gschwend, P. M. The flux of black carbon to sediments on the New England continental shelf. *Geochimica et Cosmochimica Acta*, **1998**, *62* (3), 465–472.

9. Wakeham, S. G.; Forrest, J.; Masiello, C. A.; Gélinas, Y.; Alexander, C. R.; Leavitt, P. R. Hydrocarbons in Lake Washington Sediments. A 25-year retrospective in an urban lake. *Environ. Sci. Technol.* **2004**, *38*, 431–439.

10. Louchouarn, P.; Chillrud, S. N.; Houel, S.; Yan, B.; Chaky, D.; Rumpel, C.; Largeau, C.; Bardoux, G.; Walsch, D.; Bopp, R. F. Elemental and molecular evidence of soot- and char-derived black carbon inputs to New York City's atmosphere during the 20th century. *Environ. Sci. Technol*. **2007**, *41*, 82–87.

11. Husain, L.; Khan, A. J.; Ahmed, T.; Swami, K.; Bari, A.; Webber, J. S.; Li, J. Trends in atmospheric elemental carbon from 1835 to 2005. *J. Geophys. Res.* **2008**, *113*, D13102; DOI 10.1029/2007JD009398.

12. Khan, A. J.; Swami, K.; Ahmed, T.; Bari, A.; Shareef, A.; Husain, L. Determination of elemental carbon in lake sediments using a thermal-optical transmittance (TOT) method. *Atmos. Environ.* **2009**, *43*, 5989-5995.

13. Muri, G.; Wakeham, S. G.; Rose, N. L. Records of atmospheric delivery of pyrolysis derived pollutants in recent mountain lake sediments of the Julian Alps (NW Slovenia). *Environ. Poll.* **2006**, *139* (3), 461–468.

14. Elmquist, M.; Zdenek, Z.; Gustafsson, Ö. A 700 year sediment record of black carbon and polycyclic aromatic hydrocarbons near the EMEP air monitoring station in Aspvreten, Sweden. *Environ. Sci. Technol.* **2007**, *41* (20), 6926–6932.

15. Bogdal, C.; Bucheli, T. D.; Agarwal, T.; Anselmetti, F. S.; Blum, F.; Hungerbühler, K.; Kohler, M.; Schmid, P.; Scheringer, M.; Sobek, A. Contrasting temporal trends and relationships of total organic carbon, black carbon, and polycyclic aromatic hydrocarbons in rural low-altitude and remote high-altitude lakes. *J. Environ. Monit.* **2011**, *13*, 1316–1326; DOI 10.1039/c0em00655f.

16. Sánchez-García, L.; de Andrés, J. R.; Gélinas, Y.; Schmidt, M. W. I.; Louchouarn, P. Different pools of black carbon in sediments from the Gulf of Cádiz (SW Spain): Method comparison and spatial distribution. *Marine Chemistry* **2013**, 151, 13–22.

17. Han, Y. M.; Cao, J. J.; Yan, B. Z.; Kenna, T. C.; Jin, Z. D.; Cheng, Y.; Chow, J. C.; An, Z. S. Comparison of elemental carbon in lake sediments measured by three different methods and 150-year pollution history in Eastern China. *Environ. Sci. Technol*. **2011**, *45*, 5287-5293.

18. Liu, X.; Xu, L.; Sun, L.; Liu, F.; Wang, Y.; Yan, H.; Liu, Y.; Luo, Y.; Huang, J. A 400-year record of black carbon flux in the Xisha archipelago, South China Sea and its implication. *Marine Pollution Bulletin* **2011**, *62* (10), 2205–2212.

562 19. Cong, Z.; Kang, S.; Gao, S.; Zhang, Y.; Li, Q.; Kawamura, K. Historical Trends of
563 Atmospheric Black Carbon on Tibetan Plateau As Reconstructed from a 150-Year Lake
564 Sediment Record. *Environ. Sci. Technol.* **2013**, *47* (6), 2579–2586.

565 20. Novakov, T.; Ramanathan, V.; Hansen, J. E.; Kirchstetter, T. W.; Sato, M.; Sinton, J. E.;
566 Satahye, J. A. Large historical changes of fossil-fuel black carbon aerosols. *Geophys. Res. Lett*.
567 **2003**, *30* (6), 1324; DOI 10.1029/2002GL016345.

568 21. Bond, T. C.; Bhardwaj, E.; Dong, R.; Joghani, R.; Jung, S.; Roden, C.; Streets, D. G.;
569 Trautmann, N. M. Historical emissions of black carbon and organic carbon aerosol from energy-
570 related combustion, 1850-2000. *Glob. Biogeochem. Cycles* **2007**, *21*, GB2018; DOI
571 10.1029/2006GB002840.

572 22. Clarke, A. D.; Noone, K. J. Soot in the Arctic snowpack: A cause for perturbations in
573 radiative transfer, *Atmos. Environ.* **1985**, *19*, 2045–2053.

574 23. Hansen, J.; Nazarenko, L. Soot climate forcing via snow and ice albedos. *Proc. Nat. Acad.*
575 *Sci. USA* **2004**, *101*, 423–428; DOI 10.1073/pnas.2237157100.

576 24. AMAP, 2011. The Impact of Black Carbon on Arctic Climate. By: Quinn, P.K.; Stohl, A.;
577 Arneth, A.; Berntsen, T.; Burkhart, J. F.; Christensen, J.; Flanner, M.; Kupiainen, K.;
578 Lihavainen, H.; Shepherd, M.; Shevchenko, V.; Skov, H.; Vestreng, V. *Arctic Monitoring and*
579 *Assessment Programme (AMAP)*, **2011**, Oslo, Norway. 72 pp.

580 25. Warren, S. G.; Wiscombe, W. J. A model for the spectral albedo of snow. II: Snow
581 containing atmospheric aerosols. *J. Atmos. Sci*. **1980**, *37*, 2734–2745.

582 26. Sharma, S.; Ishizawa, M.; Chan, D.; Lavoué, D.; Andrews, E.; Eleftheriadis, K.; Maksyutov,
583 S. 16-year simulation of Arctic black carbon: Transport, source contribution, and sensitivity
584 analysis on deposition. *J. Geophys. Res. Atmos*. **2013**, *118*, 943–964; DOI
585 10.1029/2012JD017774.

586 27. Wang, Q.; Jacob, D. J.; Fisher, J. A.; Mao, J.; Leibensperger, E. M.; Carouge, C. C.; Le
587 Sager, P.; Kondo, Y.; Jimenez, J. L.; Cubison, M. J.; Doherty, S. J. Sources of carbonaceous
588 aerosols and deposited black carbon in the Arctic in winter-spring: implications for radiative
589 forcing. *Atmos. Chem. Phys*. **2011**, *11*, 12453–12473; DOI 10.5194/acp-11-12453-2011.

590 28. Cozic, J.; Verheggen, B.; Mertes, S.; Connolly, P.; Bower, K.; Petzold, A.; Baltensperger, U.;
591 Weingartner, E. Scavenging of black carbon in mixed phase clouds at the high alpine site
592 Jungfraujoch. *Atmos. Chem. Phys.* **2007**, *7*, 1797–1807; DOI 10.5194/acp-7-1797-2007.

593 29. McConnell, J. R.; Edwards, R.; Kok, G. L.; Flanner, M. G.; Zender, C. S.; Saltzman, E. S.;
594 Banta, J. R.; Pasteris, D. R.; Carter, M. M.; Kahl, J. D. W. 20th century industrial black carbon
595 emissions altered arctic climate forcing. *Science* **2007**, *317*, 1381–1384; DOI
596 10.1126/science.1144856.

597 30. McConnell, J.R.; Edwards, R. Coal burning leaves toxic heavy metal legacy in the Arctic.
598 *Proc. Natl. Acad. Sci. USA* **2008**, *105*, 12140–12144; DOI 10.1073/pnas.0803564105.

599 31. McConnell, J. R. New Directions: Historical black carbon and other ice core aerosol records
600 in the Arctic for GCM evaluation. *Atmos. Environ*. **2010**, *44*, 2665–2666.

601 32. Keegan, K. M.; Albert, M. R.; McConnell, J. R.; Baker, I. Climate change and forest fires
602 synergistically drive widespread melt events of the Greenland Ice Sheet. *Proc. Natl. Acad. Sci.*
603 *USA* **2014**, *111*, 7964–7967; DOI 10.1073/pnas.1405397111.

604 33. Ruppel, M. M.; Isaksson, E.; Ström, J.; Beaudon, E.; Svensson, J.; Pedersen, C. A.; Korhola,
605 A. Increase in elemental carbon values between 1970 and 2004 observed in a 300-year ice core
606 from Holtedahlfonna (Svalbard). *Atmos. Chem. Phys*. **2014**, *14*, 11447–11460; DOI 10.5194/acp-
607 14-11447-2014.

608 34. Stohl, A. Characteristics of atmospheric transport into the arctic troposphere. *J. Geophys.*
609 *Res*. **2006**, *111*, D11306; DOI 10.1029/2005JD006888.

610 35. Hirdman, D.; Sodemann, H.; Eckhardt, S.; Burkhart, J. F.; Jefferson, A.; Mefford, T.; Quinn,
611 P. K.; Sharma, S.; Ström, J.; Stohl, A. Source identification of short-lived air pollutants in the
612 Arctic using statistical analysis of measurement data and particle dispersion model output.
613 *Atmos. Chem. Phys.* **2010**, *10,* 669–693; DOI10.5194/acp-10-669-2010.

614 36. Gustafsson, Ö.; Bucheli, T. D.; Kukulska, Z.; Andersson, M.; Largeau, C.; Rounzaud, J.-N.;
615 Reddy, C. M.; Eglinton, T. I. Evaluation of a protocol for the quantification of black carbon in
616 sediments. *Glob. Biogeochem. Cycles*, **2001**, *15* (4), 881–890.

617 37. Elmquist, M.; Cornelissen, G.; Kukulska, Z.; Gustafsson, Ö. Distinct oxidative stabilities of
618 char versus soot black carbon: Implications for quantification and environmental recalcitrance.
619 *Glob. Biogeochem. Cycles* **2006**, *20* (2), GB2009; DOI 10.1029/2005GB002629.

620 38. Hammes, K.; Schmidt, M. W. I.; Smernik, R. J.; Currie, L. A.; Ball, W. P. et al. Comparison
621 of quantification methods to measure fire-derived (black/elemental carbon in soils and sediments
622 using reference materials from soil, water, sediment and the atmosphere. *Glob. Biogeochem.*
623 *Cycles*, **2007**, *21*, GB3016; DOI 10.1029/2006GB002914.

624 39. Ruppel, M.; Lund, M. T.; Grythe, H.; Rose, N. L.; Weckström, J.; Korhola, A. Comparison
625 of spheroidal carbonaceous particle (SCP) data with modelled atmospheric black carbon

626 concentration and deposition, and air mass sources in northern Europe, 1850–2010. *Advances in*
627 *Meteorology* **2013**, 393926, 15 pages; DOI 10.1155/2013/393926.

628 40. Renberg, I.; Hansson, H. The HTH sediment corer. *J. Paleolimnol*. **2008**, *40*, 655–659.

629 41. Rose, N. L. A note on further refinements to a procedure for the extraction of carbonaceous
630 fly-ash particles from sediments. *J. Paleolimnol*. **1994**, *11*, 201–204.

631 42. Rose, N. L.; Harlock, S.; Appleby, P. G. The spatial and temporal distribution of spheroidal
632 carbonaceous fly–ash particles (SCP) in the sediment records of European mountain lakes.
633 *Water, Air, and Soil Pollution*, **1999**, *113* (1-4), 1–32.

634 43. Rose, N. L. Quality control in the analysis of lake sediments for spheroidal carbonaceous
635 particles. *Limnol. Oceanog. Methods*. **2008**, *6*, 172–179.

636 44. Wang, R., Tao, S., Balkanski, Y., Ciais, P., boucher, O., Liu, J., Piao, S., Shen, H., Vuolo, M.
637 R., Chen, H., Chen, Y., Cozic, A., Huang, Y., Li, B., Li., W., Shen, G., Wang, B., Zhang, Y.
638 Exposure to ambient black carbon derived from a unique inventory and high-resolution model.
639 *Proc. Nat. Acad. Sci. USA* **2014**, *111* (7), 2459**–**2463; DOI 10.073/pnas.1318763111.

640 45. Hedges, J. I.; Eglinton, G.; Hatcher, P. G.; Kirchman, D. L.; Arnosti, C.; Derenne, S.;
641 Evershed, R. P.; Kögel-Knabner, I.; de Leeuw, J. W.; Littke, R.; Michaelis, W.; Rullkötter, J.
642 The molecularly-uncharacterized component of non-living organic matter in natural
643 environments. *Org. Geochem*. **2000**, *31*, 945–958.

644 46. Elmquist, M.; Gustafsson, Ö.; Andersson, P. Quantification of sedimentary black carbons
645 using the chemothermal oxidation method: An evaluation of ex situ pretreatments and standard
646 additions approaches. *Limnol. Oceanogr. Methods* **2004**, *2*, 417– 427.

647 47. Nguyen, T. H.; Brown, R. A.; Ball, W. P. An evaluation of thermal resistance as a measure of
648 black carbon content in diesel soot, wood char, and sediment. *Org. Geochem*. **2004**, *35*, 217–234.

649 48. Accardi-Dey, A. M. Black carbon in marine sediments: quanitifcation and implications for
650 the sorption of polycyclic aromatic hydrocarbons. Ph.D. Thesis, Department of Civil and
651 Environmental Engineering, MIT, 2003, 279 pp.

652 49. Blais, J. M; Kalff, J. The influence of lake morphometry on sediment focussing. *Limnol.*
653 *Oceanogr*. **1995**, *40* (3), 582-588.

654 50. Rose N.L. Spheroidal carbonaceous fly-ash particles provide a globally synchronous
655 stratigraphic marker for the Anthropocene. *Environ. Sci. Technol.* **2015,** *49*, 4155−4162.

656 51. Wik, M.; Renberg, I. Environmental records of carbonaceous fly-ash particles from fossil-
657 fuel combustion: A summary. *J. Paleolimnol*. **1996**, *15*, 193-206.

658 52. Rose, N. L.; Appleby, P. G.; Regional applications of lake sediment dating by spheroidal
659 carbonaceous particle analysis I: United Kingdom. *J. Paleolimnol*. **2005**, *34* (3), 349–361; DOI
660 10.1007/s10933-005-4925-4.

661 53. Hole, L. R., Christensen, J., Forsius, M., Nyman, M., Stohl, A., Wilson, S.: Chapter 2.
662 Sources of acidifying pollutants and Arctic Haze precursors. In *AMAP Assessment 2006:*
663 *Acidifying Pollutants, Arctic Haze, and Acidification in the Arctic*; Arctic Monitoring and
664 Assessment Programme (AMAP): Oslo 2006; pp 78–81.

665 54. Dutkiewicz, V. A.; De Julio, A. M.; Ahmed, T.; Laing, J.; Hopke, P. K.; Skeie, R. B.;
666 Viisanen, Y.; Paatero, J.; Husain, L. Forty-seven years of weekly atmospheric black carbon

667 measurements in the Finnish Arctic: Decrease in black carbon with declining emissions. *J.*
668 *Geophys. Res. – Atmos.* **2014**, *119* (12), 7667–7683; DOI 10.1002/2014JD021790.

669 55. Lee, Y. H.; Lamarque, J.-F.; Flanner, M. G.; Jiao, C.; Shindell, D. T.; Berntsen, T.; Bisiaux,
670 M. M.; Cao, J.; Collins, W. J.; Curran, M.; Edwards, R.; Faluvegi, G.; Ghan, S.; Horowitz, L.
671 W.; McConnell, J. R.; Ming, J.; Myhre, G.; Nagashima, T.; Naik, V.; Rumbold, S. T.; Skeie, R.
672 B.; Sudo, K.; Takemura, T.; Thevenon, F.; Xu, B.; Yoon, J.-H. Evaluation of preindustrial to
673 present-day black carbon and its albedo forcing from Atmospheric Chemistry and Climate Model
674 Intercomparison Project (ACCMIP). *Atmos. Chem. Phys*. **2013**, *13* (5), 2607–2634; DOI
675 10.5194/acp-13-2607-2013.

676 56. Huang, K.; Fu, J. S.; Prikhodko, V. Y.; Storey, J. M.; Romanov, A.; Hodson, E. L.; Cresko,
677 J.; Morozova, I.; Ignatieva, Y.; Cabaniss, J. Russian anthropogenic black carbon: Emission
678 reconstruction and Arctic black carbon simulation. Accepted for *J. Geophys. Res. – Atmos*.,
679 **2015**; DOI 10.1002/2015JD023358.

680 57. Forsström, S.; Isaksson, E.; Skeie, R. B.; Ström, J.; Pedersen, C. A.; Hudson, S. R.; Berntsen,
681 T. K.; Lihavainen, H.; Godtliebsen, F.; Gerland, S. Elemental carbon measurements in European
682 Arctic snow packs, *J. Geophys. Res. -Atmos*., **2013**, *118*, 13614–13627; DOI
683 10.1002/2013JD019886.

684 58. Elvidge, C. D.; Ziskin, D.; Baugh, K. E.; Tuttle, B. T.; Ghosh, T.; Pack, D. W.; Erwin, E. H.;
685 Zhizhin, M. A fifteen year record of global natural gas flaring derived from satellite data.
686 *Energies* **2009**, *2*, 595–622; DOI 10.3390/en20300595.

687 59. Stohl, A.; Klimont, Z.; Eckhardt, S.; Kupiainen, K.; Shevchenko, V. P.; Kopeikin, V. M.;
688 Novigatsky, A. N. Black carbon in the Arctic: the underestimated role of gas flaring and

residential combustion emissions. *Atmos. Chem. Phys*. **2013**, *13*, 8833–8855; DOI 10.5194/acp-13-8833-2013.

60. Weckström, J.; Snyder, J. A.; Korhola, A.; Laing, T. T.; MacDonald, G. M. Diatom inferred acidity history of 32 lakes on the Kola Peninsula, Russia. *Water, Air, and Soil Pollution* **2003**, *149*, 339–361.

61. Koch, D.; Bauer, S.; Del Genio, A.; Faluvegi, G.; McConnell, J. R.; Menon, S.; Miller, R. L.; Rind, D.; Ruedy, R.; Schmidt, G. A.; Shindel, D. Coupled aerosol-chemistry-climate twentieth century transient model investigation: Trends in short-lived species and climate responses. *J. Climate*, **2011**, *24*, 2693–2714; DOI 10.1175/2011JCLI3582.1.

62. Skeie, R. B.; Berntsen, T.; Myhre, G.; Pedersen, C. A.; Ström, J.; Gerland, S.; Ogren, J. A. Black carbon in the atmosphere and snow, from pre-industrial times until present. *Atmos. Chem. Phys.* **2011**, *11*, 6809–6836; DOI 10.5194/acp-11-6809-2011.

63. Gustafsson,Ö.; Kruså, M.; Zencak, Z.; Sheesley, R. J.; Granat, L.; Engström, E.; Praveen, P. S.; Rao, P. S. P.; Leck, C.; Rodhe, H. Brown clouds over South Asia: Biomass or fossil fuel combustion? *Science* **2009**, *323* (5913), 495–498; DOI 10.1126/science.1164857.

64. Sand, M.; Berntsen, T. K.; Seland, Ø.; Kristjánsson, J. E. Arctic surface temperature change to emissions of black carbon within Arctic or midlatitudes. *J. Geophys. Res.-Atmos*. **2013**, *118*, 1–11; DOI 10.1002/jgrd.50613.

710

711

712 **Abstract Graphic:**

713

714